RF Backscatter-Based Sensors for Structural Health Monitoring

Milutin Stanaćević*, Abeer Ahmad[†], Xiao Sha*, Akshay Athalye*, Samir Das[†], Kelly Caylor[§], Branko Glisić[‡] and Petar M. Djurić*

*Department of Electrical and Computer Engineering, Stony Brook University, Stony Brook, NY 11794

†Department of Computer Science, Stony Brook University, Stony Brook, NY 11794

‡Civil and Environmental Engineering, Princeton University, Princeton, NJ 08544

§Department of Geography, UC Santa Barbara, Santa Barbara, CA 93106

Email: milutin.stanacevic@stonybrook.edu

Abstract—There is a growing need for accurate and reliable assessment of conditions of a variety of engineering structures and for monitoring of their performance. Miniaturized, passive, backscatter-based RF sensors with embedded computational capabilities could enable advanced structural health monitoring at high fidelity and at large-scale. Specifically, these RF-powered devices, pervasively embedded and dispersed within the structural material, can sense parameters of interest throughout large volumes of instrumented structure, perform modest local computations to infer structural conditions, and communicate via backscatter modulation while consuming near-zero power. We demonstrate that the backscatter channel phase sensing enables quantification of a size of air gap between two RF sensors embedded in sand. Additionally, we demonstrate the sensitivity of the phase to the strain of the sand.

I. INTRODUCTION

The commonly used discrete sensors for structural health monitoring(SHM), such as strain gauges, vibrating wires, accelerometers, and discrete fiber optic sensors, suffer from either short lifetime as they require batteries for their operation or high installation cost [1], [2]. Wireless channel estimation, in addition to enhancing the performance of a communication link, offers a sensing modality that is amenable to monitoring the surrounding environment [3], [4]. However, existing active or passive RF sensors have some important limitations in terms of spatial resolution, scalability and deployment. For granular and long-term monitoring, RF sensors have to be integrated in a small form factor and be self-powered. Conventional RFID tags provide near-zero power operation at a small-form factor but require deployment of costly RFID readers that limit the scalability of this approach [5]–[9]. Additionally, granularity of this approach is limited by the number of wireless readerto-tag channels in this centralized system. RF sensors with active radio could provide granularity based on sensor-tosensor channel estimation, but the power requirement for an active radio prohibits the self-power operation of this type of sensors.

RF tags, as an enabling technology for low-power communication, has been established recently [10]–[12]. RF tags can talk to each other without the presence of a centralized device like a reader by way of backscattering an ambient RF signal. If the power level of an ambient RF signal is

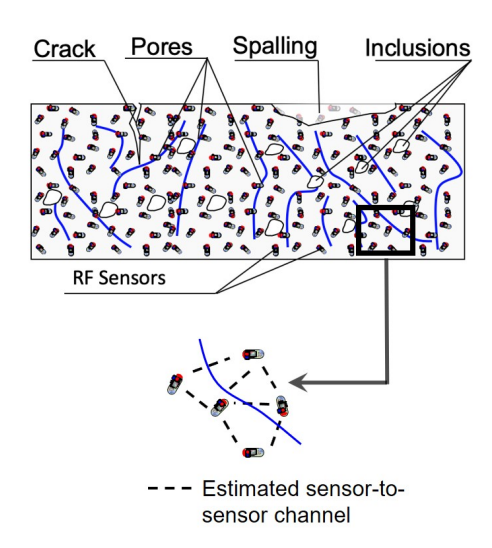


Fig. 1. Sensing system for structural health monitoring comprising a number of RF sensors embedded in a concrete structure.

not high enough for backscatter-based communication, a CW signal can be generated by a dedicated low-cost device, exciter. A RF tag with a transmitter based on a passive modulator and a receiver based on an envelope detector allows for extreme low-power cost for communication [13]–[15]. Passive RF sensing is enabled by the ability of the tags to estimate the RF parameters of the wireless channel between pairs of communicating tags without the use of IO demodulation. We have previously proposed a technique for the channel phase estimation in tag-to-tag link that estimates the joint phase of the exciter-tag channels and the tag-to-tag channel [16]-[18]. Extending the tag-to-tag backscatter communication to RFbased sensing makes the tags behave like RF sensors. We have already demonstrated that this technique can be used for activity recognition [16] and here we explore the possibility of applying these sensors to structural health monitoring.

We envision a distributed complex system comprising of numerous tiny RF sensors permanently embedded in a structure, as illustrated in Figure 1. The sensors are able to selflocalize and monitor material parameters by estimating wireless backscatter channels. The continuous, extremely fine-grain monitoring of the structure enables detection, localization, and quantification of the changes in material. In this paper, we investigate the relationship between the wireless channel parameters and properties of the channel medium material. We account for variability of a single material property, like integrity and strain in time and space, and observe changes in the properties of the wireless channel.

II. PASSIVE SENSOR-TO-SENSOR CHANNEL ESTIMATION

To demonstrate how the wireless channel can be passively estimated, we observe the signal-level operation of the sensor-to-sensor channel. We illustrate the channel estimation between two RF sensors in presence of a CW generator, exciter, as shown in Figure 2. For simplicity of the derivation, we assume a static environment. The received RF signal at each sensor is a combination of the signal originating from the exciter and the signal reflected from the other sensor. The sensor has an envelope detector that extracts the amplitude of the received signal. The amplitude of the received signal at sensor b, when the reflection coefficient of the sensor a has amplitude equal to 1 and phase equal to $\phi_{a,k}$, is denoted as $\hat{v}_{b,k}$. The amplitude of the input voltage at sensor b, when the modulator of sensor a is terminated with 50 Ω is denoted as $\hat{v}_{b,0}$. The difference between these amplitudes is

$$\hat{v}_{b,k} - \hat{v}_{b,0} = A_{Ea} A_{ab} \cos(\theta_{Ea} + \theta_{ab} + \phi_{a,k} - \theta_{Eb}), \quad (1)$$

where A_{Ea} is the amplitude of the channel exciter \rightarrow sensor a scaled by the power of the exciter, and A_{ab} is the amplitude of the channel sensor $a \rightarrow sensor b$ [16]. The symbols θ_{Ea} , θ_{ab} and θ_{Eb} are the phases of the channels $exciter \rightarrow sensor \ a, \ sensor \ a \rightarrow sensor \ b$ and $exciter \rightarrow sensor \ b$, respectively. The estimation of the amplitude and phase of the sensor-to-sensor channel is performed in the following fashion. We vary the reflection phase of the sensor a, $\phi_{a,k}$, in a span from $-\pi$ to π and for each phase record the difference between the voltages $\hat{v}_{b,k}$ and $\hat{v}_{b,0}$. By interpolation, from the sampled voltage signals, we obtain estimates of the product of amplitudes $A_{Ea}A_{ab}$ and phase $\theta_{a2b,est} = -\theta_{Ea} - \theta_{ab} + \theta_{Eb}$. We note that this is not the amplitude and phase of the sensor-to-sensor channel, as it includes the properties of the channel from exciter to both sensors.

Similarly, if we observe the signal after the envelope detector at sensor a, we obtain that the amplitude difference between two impedance states at sensor b is equal to

$$\hat{v}_{a,k} - \hat{v}_{a,0} = A_{Eb} A_{ab} \cos(\theta_{Eb} + \theta_{ab} + \phi_{b,k} - \theta_{Ea}), \quad (2)$$

where A_{Eb} is the amplitude of the channel $exciter \rightarrow sensor\ b$ scaled by the power of the exciter. From the measurements of the voltage differences $\hat{v}_{a,k}$ and $\hat{v}_{a,0}$ at the output of the envelope detector of sensor a, for a set of reflection phases $\phi_{b,k}$, we obtain estimate of the amplitude $A_{Eb}A_{ab}$ and phase $\theta_{b2a,est} = -\theta_{Eb} - \theta_{ab} + \theta_{Ea}$.

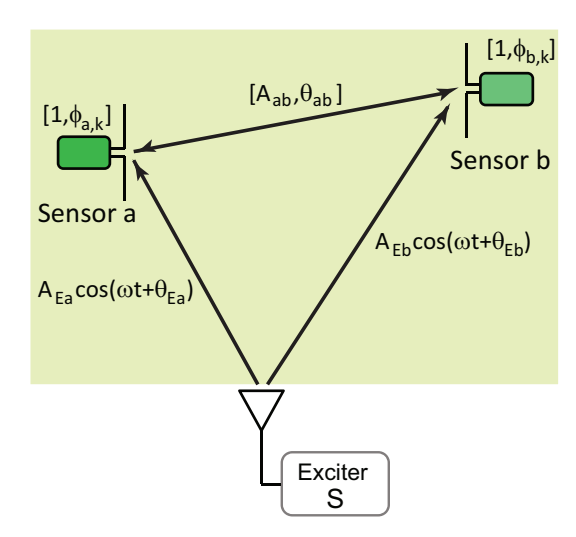


Fig. 2. Passive estimation of the amplitude and phase, $[A_{ab}, \theta_{ab}]$, of sensor-to-sensor channel.

From these two estimated phases, we can obtain the estimate of the sensor a to sensor b channel as

$$\theta_{ab,est} = -(\theta_{a2b,est} + \theta_{b2a,est})/2. \tag{3}$$

The estimated phase is independent of the $exciter \rightarrow sensor$ channel phases, θ_{Ea} and θ_{Eb} , leading to the invariance of the estimate of sensor-to-sensor channel phase, θ_{ab} , on the location of the exciter. This is particularly important for sensing applications where the RF sensors are embedded in observed material and the exciter is located in air. Similarly, we estimate the amplitude of the sensor-to-sensor channel, A_{ab} . The phase estimate is more robust and when the channel is estimated in air, due to multi-path, often only the phase is used in applications like distance measurement and localization. In our problem, we can show that the accuracy of the phase estimate is much better than it is for the amplitude. It turns out that the phase in our problem plays the role of frequency of a sinusoid, and it is well known from estimation theory that the frequency of a sinusoid can be estimated with much better accuracy than the amplitude of a sinusoid [19].

From the estimated amplitude and phase of the sensor-tosensor channel, the ratio of the distance between the sensors and wavelength is obtained, a function of the electromagnetic parameters of the medium that surrounds the sensors [20]. The electromagnetic parameters of the medium used in the propagation model are differently affected by factors like humidity and temperature, as well as the transmission frequency. We first study the relationship between the integrity and strain of a material, in this case sand, on the phase of the wireless channel.

III. EXPERIMENTAL RESULTS

To demonstrate the relationship between material properties and wireless channel between two RF sensors, we performed a set of experiments. In all the experiments, we used a discrete implementation of the RF tag, shown in Figure 3

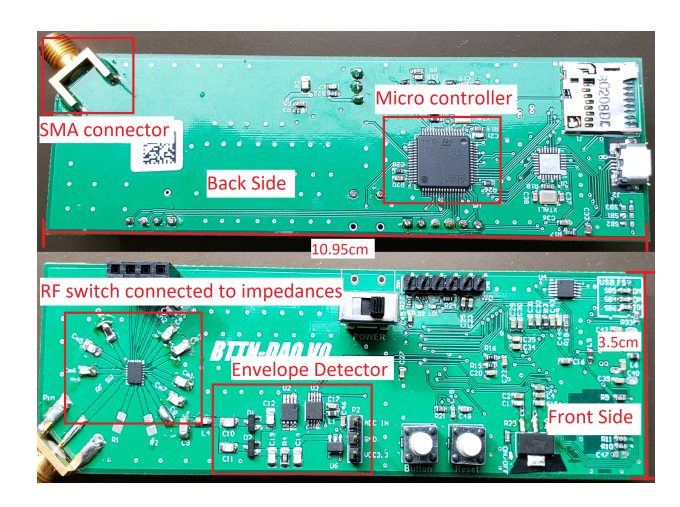


Fig. 3. Discrete implementation of an RF tag used in the experiments.

which interfaces a dipole antenna. The RF tag implemented a multiphase modulator and demodulator based on the envelope detector. The multi-phase modulator integrated a multi-port RF switch terminated, in addition to open-circuit and 50 Ω , with seven impedances, preselected to provide the phases of the reflection coefficient evenly spaced in a range of 2π . The demodulator implementation included the envelope detector followed by a low-pass filter and a 16-bit 1 MSample/s analog-to-digital (ADC) converter. The digitized amplitude of the input RF signal was then transferred to a PC for data analysis.

We first demonstrated how the phase of the wireless channel depends on the distance between the sensors in air as the medium between the sensors. The sensors were positioned on a rail and the distance was changed from 22 cm to 80 cm. The exciter antenna was positioned at distances of 2 m from the sensors. The plot of the phase as a function of the distance between the sensors is shown in Figure 4.

To examine the relationship between material properties and wireless channel, we used sand. The experimental setup is shown in Figure 5. A storage container of size 29.7"x20"x17.5" was filled with sand. The sensor antennas were fixed to the opposing walls of the container where the distance between the antennas was 50 cm. The exciter antenna with circular polarization was placed at a distance of 1 m from the side of the container and at equal distance from both sensor antennas. The source generator connected to a circularly polarized antenna provided CW signal at 915 MHz.

In the first set of experiments we introduced air gap of different widths in the sand in order to simulate the loss of integrity in the structure, e.g., due to cracking or spalling. We first measured the phase of the channel between the sensors when the container was completely filled with sand. Next, we created an air gap that was 5 cm wide in the middle of the container and measured the channel phase. The experiment was repeated with the air gap width increased by 5 cm until it became 20 cm. The phase of the channel as a function of width of the air gap is shown in Figure 6 demonstrating changes in the phase. This large gaps do not reflect real (small) sizes of

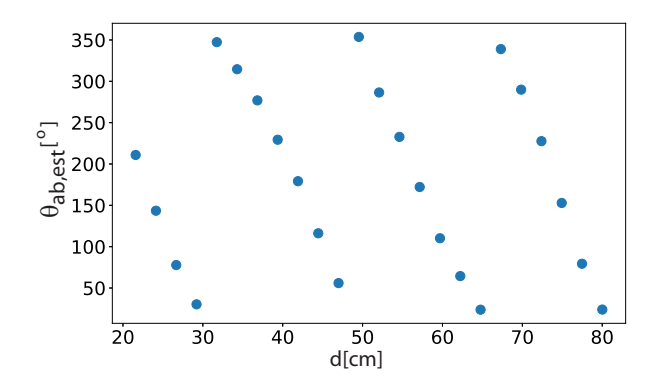


Fig. 4. Phase of the channel in air as a function of distance between the sensors.

cracks in real-world settings; however, the aim of the tests was only to prove the concept.

A second experiment was performed to demonstrate the effect of the strain on the parameters of the channel. The phase of the channel was first sampled with the storage container fully filled with sand. Then, a weight of 5 lbs was placed on top of the sand and left for one hour. The phase was sampled and the estimated phase for both cases is shown in Figure 7. Clearly, the estimated phase when there was no weight was different from the estimated phase when we applied weight of 5 lbs. We also found that the variance of the estimate in the latter case was much higher than that corresponding to the former case.

IV. CONCLUSIONS

We envision that the backscater-based RF sensor could be mixed with binding structural materials (e.g., cement, geopolymers, resins and plastic composites), or dispersed in the media (e.g., soil). Then, it could be used to evaluate and monitor material properties at macro-level such as integrity (presence of cracks and their propagation over time), internal humidity (water content in pores and its variability over time), strain and temperature. We demonstrated feasibility of sensing the phase of the wireless channel in quantifying single dynamic parameter of the material in which sensor are embedded. In future work, we will also investigate simultaneous changes of multiple observed parameters of the material.

ACKNOWLEDGMENT

This research is supported by the National Science Foundation (NSF) under grant number CNS-1763843 and CNS-1901182.

REFERENCES

- [1] A. B. Noel, A. Abdaoui, T. Elfouly, M. H. Ahmed, A. Badawy, and M. S. Shehata, "Structural health monitoring using wireless sensor networks: A comprehensive survey," *IEEE Communications Surveys & Tutorials*, vol. 19, no. 3, pp. 1403–1423, 2017.
- [2] B. Glisic, "Distributed fiber optic sensing technologies and applications an overview," *Special Publication*, vol. 292, pp. 1–18, 2013.
- [3] H. Meyr, M. Moeneclaey, and S. Fechtel, Digital Communication Receivers: Synchronization, Channel Estimation, and Signal Processing. John Wiley & Sons, Inc., 1997.



Fig. 5. Experimental setup. Left: Side view of the antenna which is fixed to the side of the container. Right: Top view showing the air gap in the channel.

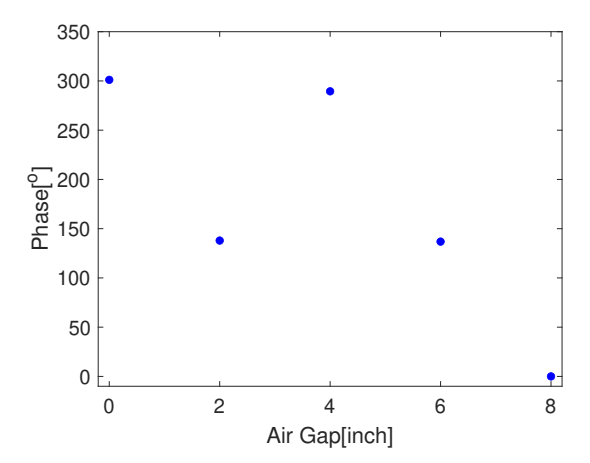


Fig. 6. The phase of the RF sensor-to-sensor channel as a function of the air gap width created between the sensors.

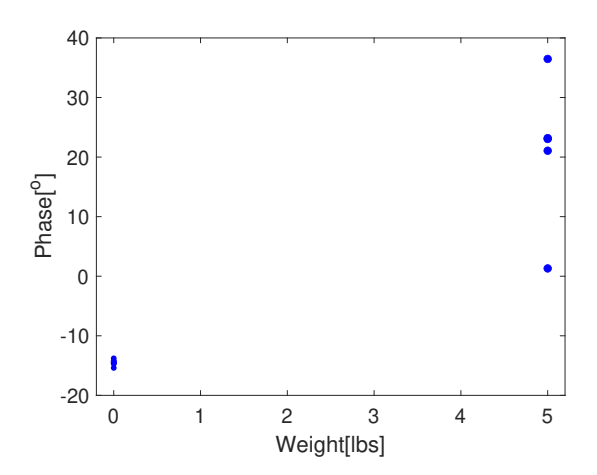


Fig. 7. The phase of the RF sensor-to-sensor channel as a function of weight applied to the top of the sand.

- [4] Y. Li, N. Seshadri, and S. Ariyavisitakul, "Channel estimation for OFDM systems with transmitter diversity in mobile wireless channels," *IEEE Journal on Selected Areas in Communications*, vol. 17, no. 3, pp. 461–471, 1999.
- [5] S. Kim, C. Mariotti, F. Alimenti, P. Mezzanotte, A. Georgiadis, A. Collado, L. Roselli, and M. M. Tentzeris, "No battery required: Perpetual

- RFID-enabled wireless sensors for cognitive intelligence applications," *IEEE Microwave Magazine*, vol. 14, no. 5, pp. 66–77, 2013. A. P. Sample, D. J. Yeager, P. S. Powledge, A. V. Mamishev, and J. R.
- [6] A. P. Sample, D. J. Yeager, P. S. Powledge, A. V. Mamishev, and J. R. Smith, "Design of an RFID-based battery-free programmable sensing platform," *IEEE Transactions on Instrumentation and Measurement*, vol. 57, no. 11, pp. 2608–2615, 2008.
- [7] D. Yeager, A. Sample, and J. Smith, "Wisp: A passively powered UHF RFID tag with sensing and computation," *RFID Handbook: Applica*tions, Technology, Security, and Privacy, pp. 261–278, 2008.
- [8] H. Zhang, J. Gummeson, B. Ransford, and K. Fu, "Moo: A batteryless computational RFID and sensing platform," *University of Massachusetts Computer Science Technical Report UM-CS-2011-020*, 2011.
- [9] M. Buettner, B. Greenstein, and D. Wetherall, "Dewdrop: an energy-aware runtime for computational RFID," in *Proc. USENIX NSDI*, 2011, pp. 197–210.
- [10] V. Liu, A. Parks, V. Talla, S. Gollakota, D. Wetherall, and J. R. Smith, "Ambient backscatter: Wireless communication out of thin air," ACM SIGCOMM Computer Communication Review, vol. 43, no. 4, pp. 39– 50, 2013.
- [11] A. N. Parks, A. Liu, S. Gollakota, and J. R. Smith, "Turbocharging ambient backscatter communication," ACM SIGCOMM Computer Communication Review, vol. 44, no. 4, pp. 619–630, 2014.
- [12] J. Ryoo, J. Jian, A. Athalye, S. R. Das, and M. Stanaćević, "Design and evaluation of "BTTN": a backscattering tag-to-tag network," *IEEE Internet of Things Journal*, vol. 5, no. 4, pp. 2844–2855, 2018.
- [13] C. Boyer and S. Roy, "Backscatter communication and RFID: Coding, energy, and mimo analysis," *IEEE Transactions on Communications*, vol. 62, no. 3, pp. 770–785, 2014.
- [14] J. Griffin and G. Durgin, "Complete link budgets for backscatterradio and RFID systems," *IEEE Trans. on Antennas and Propagation Magazine*, vol. 51, no. 2, pp. 11–25, 2009.
- [15] Y. Karimi, A. Athalye, S. Das, P. M. Djurić, and M. Stanaćević, "Design of backscatter-based tag-to-tag system," in *IEEE International Conference on RFID (RFID)*, 2017.
- [16] J. Ryoo, Y. Karimi, A. Athalye, M. Stanaćević, S. R. Das, and P. M. Djurić, "BARNET: Towards activity recognition using passive backscattering tag-to-tag network," in *Proceedings of the 16th Annual International Conference on Mobile Systems, Applications, and Services*. ACM, 2018, pp. 414–427.
- [17] Y. Karimi, Y. Huang, A. Athalye, S. Das, P. M. Djurić, and M. Stanaćević, "Passive wireless channel estimation in RF tag network," in 2019 IEEE International Symposium on Circuits and Systems (IS-CAS). IEEE, 2019, pp. 1–5.
- [18] M. Stanaćević, A. Athalye, Z. Haas, S. Das, and P. M. Djurić, "Backscatter communications with passive receivers: From fundamentals to applications," *ITU Journal*, vol. 1, no. 1, 2020.
- [19] S. M. Kay, Modern Spectral Estimation: Theory and Application. Pearson, 1988.
- [20] R. Fletcher, U. P. Marti, and R. Redemske, "Study of uhf rfid signal propagation through complex media," in 2005 IEEE Antennas and Propagation Society International Symposium, vol. 1. IEEE, 2005, pp. 747–750.